

METHOD AND APPARATUS FOR IN SITU DEPOSITING OF NEUTRAL CS
UNDER ULTRA-HIGH VACUUM TO ANALYTICAL ENDS

5

Field of the invention

[0001] The present invention relates to a new Secondary Ion Mass Spectroscopy (SIMS) method operating in the MCs_x^+ ($x = 1, 2$) mode. The method has been carried out
10 in a Cation Mass Spectrometer (CMS) developed and modified by the inventors for reaching high secondary emission useful yields combined with excellent depth and lateral resolution.

[0002] The invention also relates to the modified
15 CMS, in particular by means of a cesium deposition column which is coupled with traditional primary bombardment column.

Prior art and related technical background

20 [0003] Owing in particular to its excellent sensitivity and its good depth resolution, Secondary Ion Mass Spectrometry (SIMS) constitutes an extremely powerful technique for analysis of surfaces and thin films. Its main fields of application lie in the semiconductor, glass,
25 organic and metallurgical composite materials.

[0004] SIMS instruments also allow the recording of ion images of the surface of the analysed sample. In this case, a thin ion probe sweeps the surfaces of the sample and the secondary ions which have suitably selected mass
30 are recorded with respect to the position on the surface from which they originate. An emerging field of application for this imaging technique providing good lateral resolution combined with excellent sensitivity is situated in particular in biology.

[0005] Alongside all its advantages, however, the SIMS technique suffers from one major drawback: the measurements can only be quantified with difficulty. The intensity of the measured signals is generally greatly dependent on the sample analysed, given that the ionisation yield of a given sputtered element may vary by several orders of magnitude depending on the composition of the matrix in which it is located. This phenomenon is known as the matrix effect.

10 [0006] In order to get round these problems linked to the matrix effect, the SIMS analyses are increasingly carried out in MCs_x^+ mode. This method consists in incorporating cesium (Cs) in the material of interest and detecting positive ion clusters formed by the recombination of an atom of the element M in which one is interested together with one or two atoms of Cs. Given that these MCs_x^+ clusters are formed by atomic recombinations above the surface of the sample, the composition of the matrix does not come any longer into play directly, consequently eliminating the matrix effect.

[0007] SIMS instruments of prior art have exclusively used a beam made of Cs^+ primary ions in order to perform analyses in the MCs_x^+ mode. A number of drawbacks are still to be listed with this respect.

25 Optimisation of the Cs concentration to form MCs_x^+ clusters

[0008] When the analyses in MCs_x^+ mode are carried out by bombarding the sample with a beam of Cs^+ ions, this beam serves both for the incorporation of Cs in the material and for the sputtering of the surface. In this case, the Cs concentration, which is a crucial parameter determining the sensitivity of the analysis, as shown in figure 1, is set by the primary bombardment conditions - mainly the angle and energy of impact- which can be adapted

only in a very limited way on conventional SIMS equipment. Consequently, the Cs concentration is practically fixed for a given type of sample and cannot be chosen freely. As it is unlikely that the Cs concentration thus obtained will
5 coincide with the optimum concentration for the material in question, the analysis is not optimised.

Coupling of the Cs concentration and the depth resolution

[0009] A second major disadvantage of the use of Cs⁺ ion bombardment relates to the impossibility of separately
10 choosing the Cs concentration (c_{Cs}) implanted in the sample and the energetic and angular parameters of the primary beam, given that the latter determine the value of c_{Cs} . Now the primary bombardment conditions also considerably affect major analytical characteristics such as the depth
15 resolution.

Pre-equilibrium state

[0010] The introduction of Cs into the material by ion bombardment does not allow an optimum Cs concentration to be attained right from the first atomic layer, given
20 that the Cs atoms are implanted under the surface, as shown in figure 2, at greater or lesser depth depending on their impact energy. Consequently, the analysis is inconclusive in the pre-equilibrium state which precedes the achieving of a constant concentration of Cs (in a Cs⁺ bombardment) or
25 Cs and Ga (in a Cs⁺ and Ga⁺ bombardment).

Optimisation of formation of negative secondary ions

[0011] Furthermore, bombardments by electropositive elements are often used to raise the negative ion yield by several orders of magnitude. In this context, the emission
30 of negative secondary ions is greatly enhanced by the presence of Cs atoms on the surface of the sample which is bombarded.

Aims of the invention

[0012] The present invention aims at providing a new Secondary Ion Mass Spectroscopy (SIMS) method operating in the MCS_x^+ ($x = 1, 2$) mode permitting to separately choose the Cs concentration implanted in the sample and the sputtering of the sample surface, leading thus to simultaneous optimisation of the Cs concentration and analytical parameters, such as depth resolution, which depend now exclusively on primary bombardment conditions.

10 [0013] Particularly, the invention aims at permitting one, by depositing neutral Cs atoms on the sample surface, to vary the Cs concentration continuously in the range quasi 0 to 100% to an optimum value in order to maximise detected MCS_x^+ and Cs_x^+ signals for any kind of sample.

[0014] Additionally, the invention aims at enabling an optimised signal to be measured right from the first atomic layer.

[0015] Another goal of the present invention is to provide a specially-developed cesium column with significant service life increase and designed to considerably reduce the risk of contaminating of the cesium deposit as well as of the analysis chamber with traces of other elements.

25

Summary of the invention

[0016] A first object of the present invention relates to a method for modifying the electronic properties of a surface to analytical ends, characterised in that it comprises in situ deposition of neutral cesium (Cs^0), under ultra-high vacuum (residual pressure of about 10^{-9} - 10^{-10} mbar), said neutral cesium being enabled in the form of a collimated adjustable stream.

30

[0017] According to the invention, the stream of Cs^0 is provided and collimated in a column by means of:

- a temperature adjustment of an evaporator comprising a metallic cesium reservoir, and/or
- 5 - an aperture control of a motorised obturator located in the path of the cesium stream.

[0018] It was particularly contemplated by the inventors that said Cs^0 deposition be simultaneously accompanied by a primary bombardment comprising electrons
 10 and/or ions or neutral atoms or groups of atoms, or by an X-ray irradiation, intended to induce an emission of a beam of particles for analysis, out of the surface.

[0019] Preferably, the method of the invention is coupled to static or dynamic Secondary Ion Mass
 15 Spectroscopy (SIMS), preferably operating in the MCS_x^+ mode ($x = 1, 2$).

[0020] Advantageously, the deposition rate of Cs^0 is continuously adjustable in the range from 0 to 10 Å/s, corresponding about to 0 - 4 monolayers per second.

20 [0021] According to another preferred embodiment, the method of the invention is coupled to electron spectroscopy, preferably Auger Electron Spectroscopy (AES), Electron Energy Loss Spectroscopy (EELS), X-Ray Photoemission Spectroscopy (XPS) or Ultraviolet
 25 Photoemission Spectroscopy (UPS).

[0022] According to the SIMS embodiment, the secondary beam for analysis comprises secondary electrons and/or Cs_x^{n+} and/or MCS_x^{n+} positive clusters and/or M^{n-} negative ions and/or M^{m+} positive ions, M being a
 30 constituent of the sample material made of an atom or a group of atoms (n, m integers).

[0023] Advantageously, the sputtering and Cs introduction phases are decoupled during analyses in the

MCs_x⁺ mode, in a simultaneous optimisation of deposited Cs concentration and analytical characteristics, such as the depth resolution.

5 [0024] Still more advantageously, the depth resolution solely depends on the bombardment conditions for the analysis.

[0025] The method of the invention further enables a stream of a chemical element other than Cs, evaporated under ultra-high vacuum, to create secondary emission for
10 analytical purposes of M₁M₂ⁿ⁺ clusters or M₂^{m-} ions or M₂^{m+} ions (n, m integers) or electrons, wherein M₁ and M₂ are respectively the atoms or groups of atoms constituted by the chemical element other than Cs and the atoms or groups of atoms from the sample.

15 [0026] Still advantageous, the sole adjustable deposition rate of Cs⁰ or a chemical element other than Cs to an optimised value enables to optimise the intensity of the secondary particles emitted by the sample.

[0027] According to a preferred embodiment, the
20 reservoir temperature range is maintained between 70 and 90 °C, corresponding to a pressure range from 1.10⁻⁴ to 4.10⁻⁴ mbar and in that the stability of the deposition rate is about 2% over 60 minutes.

[0028] Under bombardment analysis mode, the
25 deposited Cs⁰ concentration is solely related to the respective Cs and sample densities (ρ_{Cs}, ρ_M), to the sputtering yield in the given bombardment conditions (Y) and to the ratio between the Cs⁰ erosion (v_{er}) and the deposition (v_D) rate (τ = v_{er}/v_D).

30 [0029] A significant advantage of the invention resides in the fact that the useful yield, i.e. the sensitivity, of the secondary emission species, preferably Mⁿ⁻, M^{m+}, and still more preferably Cs_xⁿ⁺ and MCs_xⁿ⁺, is

approximately solely related to said ratio (τ) and not to the respective erosion and deposition rate taken individually and in that the secondary signal is optimisable by adjusting the Cs^0 deposition rate to attain
5 an optimum value of said ratio (τ).

[0030] Preferably, the stream of Cs^0 is automatically and continuously adapted via the obturator.

[0031] A second object of the invention relates to an energy and/or mass analyser instrument, for carrying out
10 the method described, comprising a neutral cesium (Cs^0) deposition column capable of delivering an adjustable and stable stream of pure neutral cesium, said column being preferably usable simultaneously with a primary bombardment or a primary irradiation column.

15 [0032] The instrument preferably is a static or dynamic secondary ion mass spectrometry (SIMS) instrument, comprising a primary bombardment column and a secondary column equipped with secondary ion extraction means, a mass spectrometer, preferably of the type TOF (Time-Of-Flight),
20 quadrupolar or with magnetic sector and ion detection means.

[0033] A third object of the invention relates to a neutral cesium column usable in an instrument, such as described. The neutral cesium column comprises an
25 evaporation block including a reservoir filled with pure metallic cesium, equipped with temperature control means, prolonged by a tube up to a gun end piece located close to the sample and equipped with beam collimation means.

[0034] Advantageously, said beam collimation means
30 comprise a motorised continuously adjustable obturator, preferably comprising a rotary disk using a slit of continuously variable width, said disk being driven by a stepper motor.

[0035] Still advantageously, at the operation temperature, the neutral cesium (Cs^0) is in liquid state and the evaporation block lies with an inclination angle such as said liquid remains in the bottom of the reservoir under gravity effect.

[0036] Still advantageously, said tube and gun end piece equipped with beam collimation means are further equipped with temperature control means for preventing condensation and obturation risks.

10 [0037] Preferably, the evaporator bloc is located in an external part which can be isolated from the main chamber of the instrument by means of a gate valve and capable of being separately pumped and vented.

15 **Short description of the drawings**

[0038] FIG.1 represents the evolution of useful yields (i.e. sensitivity) as a function of the Cs concentration for the aluminium sample (Cs^+ or Cs^+/Ga^+ primary ion bombardment).

20 [0039] FIG.2 represents the depth evolution of Cs concentration implanted in a silicon sample for two different modes of analysis : pure Cs^+ bombardment and Cs^+/Ga^+ co-bombardment.

[0040] FIG.3 represents the principle of analyses grouping together the sputtering and Cs incorporation stages (a) and those separating these two stages (b).

[0041] FIG.4 comparatively represents the depth evolution of the Cs concentration in silicon for three different modes of analysis : pure Cs^+ bombardment, Cs^+/Ga^+ co-bombardment and Ga^+ bombardment with Cs^0 deposition, the latter corresponding to the difference with figure 2.

30 [0042] FIG.5 represents a schematic overall view of the Cs^0 evaporator of the invention, wherein the external and internal parts are separated at the gate valve.

[0043] FIG.6 represent a schematic representation of a preferred obturator embodiment.

[0044] FIG.7 represents the change in the Cs^0 deposition rate on the sample as a function of the heating power transmitted to the neutral cesium reservoir.

[0045] FIG.8 represents the change in the Cs^0 deposition rate onto the sample as a function of the temperature (in mV) of said reservoir.

[0046] FIG.9 represents the fluctuation of the Cs^0 deposition rate indicated by the quartz microbalance controller over a one-hour period for a reservoir heating power of 85 W. The solid line indicates the average value.

[0047] FIG.10 represents the profile of the Cs^0 beam recorded by determining the deposition rate for different positions of the quartz balance. The abscissa 0 corresponds to the position located directly below the secondary ion extraction nose. The continuous curve approximates the experimental points by a Gaussian.

[0048] FIG.11 represents the variation of the Cs concentration determined experimentally for four different Cs^0 deposition rates with respect to different erosion rates for an aluminium sample.

[0049] FIG.12 represents the experimental change (squares) and theoretical change (solid curve) of the Cs concentration as a function of the parameter τ for the aluminium sample.

[0050] FIG.13 represents the change in the useful yield of the sputtered AlCs_2^+ cluster of a sample of aluminium as a function of the characteristic parameter τ .

[0051] FIG.14 represents the SIMS depth profile of a sample of Si subjected to an implantation of Mg and In.

[0052] FIG.15 represents the SIMS depth profile of a Al sample subjected to an implantation of Ti and Cu.

[0053] FIG.16 represents the SIMS depth profile of a sample of InP subjected to an implantation of F and Al.

[0054] FIG.17 respectively represents AlCs^+ , CuCs^+ , Cs^+ and Cs_2^+ secondary ion images of the same area of an
5 Al/Cu grid.

Description and advantages of the invention

[0055] The Laboratory for the Analysis of Materials (LAM) of the Centre de Recherche Public - Gabriel Lippmann
10 has developed and installed on the Cation Mass Spectrometer (CMS), which is a prototype scientific instrument [1,2], a column which allows an adjustable and collimated stream of neutral cesium (Cs^0) to be deposited on the surface of the material sample to be analysed.

15 [0056] Using this new column, it was possible to introduce an analysis technique consisting of a $\text{X}^{\text{Y}+}$ ion bombardment accompanied by a deposit of Cs^0 at the surface of the sample. This experimental technique permits to avoid the constraints imposed by a Cs^+ ion bombardment which were
20 described above in the prior art section.

[0057] This new analysis technique provides an additional degree of freedom by separating the sputtering and Cs introduction phases of analyses in MCs_x^+ mode with aiming at a simultaneous optimisation of the Cs
25 concentration and of the major analytic characteristics such as the depth resolution which mainly depend on the primary bombardment conditions. The principle of the invention is roughly illustrated in figure 3.

[0058] When the optimum quantity of Cs is deposited
30 in the form of neutral atoms on the surface of the sample, no sputtering process or atomic mixing of the target takes place and the depth resolution of the analysis depends, advantageously, solely on the characteristic conditions of the bombardment produced by the sputtering/analysis gun.

[0059] On the other hand, the use of the Cs evaporator which deposits the Cs atoms right from the surface of the sample enables an equilibrium state to be attained from the first atomic layer, as shown in figure 4.

5 This new analysis technique therefore offers a considerable advantage in the analysis of samples in which the interesting zone is in the close vicinity of the surface.

[0060] Finally, this same Cs⁰ column also enables optimisation of the negative secondary ions by depositing
10 the optimum quantity of Cs.

[0061] References:

[1] T. Mootz, B. Rasser, P. Sudraud, E. Niehuis, T. Wirtz, W. Bieck, H.-N. Migeon, in A. Benninghoven, P. Bertrand, H.-N. Migeon, H.W. Werner (Eds.), Secondary Ion
15 Mass Spectrometry SIMS XII, Elsevier, Amsterdam, 2000, p. 233-236.

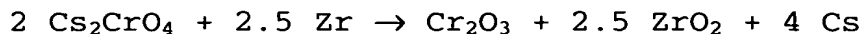
[2] T. Wirtz, B. Duez, H.-N. Migeon, H. Scherrer, Int. J. Mass Spectrom. 209 (2001) 57.

20 Description of a preferred embodiment of the invention

1.The Cs⁰ evaporator

1.1. Operating principle

[0062] To deposit alkaline metals, laboratories almost exclusively use getters, marketed by the Italian
25 group SAES, containing the alkaline metal X in the form of chromate X₂CrO₄ and a Zr_xAl_y type powder acting as a reducing agent in order to release the X (i.e. Cs) atoms. When this mixture is heated by circulating an electric current, the reduction reaction is activated and the
30 quantity of alkaline atoms thus produced depends on the heating power. In the case of Cs, this reduction reaction is written as follows:



[0063] The use of such a getter on the CMS machine to carry out the optimisations cited here above nevertheless presents several major drawbacks. First of all, preliminary calculations have shown that, in standard bombardment conditions, a Cs deposition rate of approximately 1 Å/s would be appropriate. To attain such a stream of Cs atoms on the surface of the sample while at the same time choosing an acceptable source-sample distance, it is necessary for the getter to emit at a rate of approximately $4 \cdot 10^{14}$ atoms/s, which corresponds to $8.8 \cdot 10^{-8}$ g/s. Now as a 1 cm-long getter is filled with 4.4 mg of Cs and such a length may not be exceeded in order to guarantee that the majority of the Cs atoms are deposited in the zone to be analysed, the Cs source would have a service life of only $5 \cdot 10^4$ s or 14 hours. As the stream of Cs atoms is not collimated and therefore covers a much bigger space than necessary, the service life calculated in this way represents a theoretical upper limit.

[0064] The impossibility of directing the Cs stream exclusively onto the analysis zone is a second major disadvantage of getters. In addition to the considerable loss of useful Cs atoms, such an uncollimated emission is also very likely to contaminate the whole analysis chamber by depositing a conductive and highly reactive film on all the surfaces, including ceramics serving as electrical insulators which will thereby be rendered ineffective.

[0065] Finally, the vapours emitted by commercial getters always contain traces of other elements originating mainly in the reducing agents used. This contamination of the Cs deposit is likely to increase the detection limits for certain elements given that the signal of the element

in question would be affected by a background noise of varying degrees of intensity.

[0066] In view of these service life drawbacks, contamination of the analysis chamber and cleanliness of the Cs deposit, we decided not to use a conventional getter to equip the CMS machine of the invention.

[0067] As an alternative, we developed a source emitting a stream of Cs from the evaporation of pure metallic Cs. This configuration was intended to enable the elimination of at least the first two major disadvantages of conventional getters mentioned above. Indeed, the service life can be increased enormously (by a factor of 1000) given that it is possible to fill the reservoir with a large quantity of Cs (several grams) and given that the Cs beam can be collimated on the useful zone by using a gun end piece with a small opening positioned close to the sample. Finally, as the evaporator is loaded with pure metallic Cs, the risk of contaminating the Cs deposit with traces of other elements is also reduced.

20 1.2. Description

[0068] The Cs evaporator specially designed for the CMS machine of the invention comprises two separate parts, as shown in figure 5. While the first part is located completely inside the main chamber of the CMS instrument, the second part is mounted outside the chamber using a 40CF flange. Because of their respective positions with respect to the main chamber, the two parts will henceforth be referred to as the "internal" and "external" parts.

1.2.1. External part

30 [0069] The external part of the evaporator comprises an actual evaporation block 1 and a tube (primary tube 2) guiding the stream of gaseous Cs towards the internal part of the evaporator. It can be isolated from the main chamber

3 of the CMS machine by means of a gate valve 4 and be independently pumped or vented.

[0070] The evaporation block 1 is a solid cast stainless steel part. This block contains a cylindrical housing in which the reservoir 5 containing the metallic Cs slides. The maximum capacity of this reservoir is 7.6 g of Cs. To prevent the liquid Cs from flowing out into the whole volume of the evaporator, the evaporation block is mounted on the external part of the evaporator with an angle of inclination such that all the liquid Cs remains at the bottom of the reservoir under the effect of gravity. To obtain gaseous Cs, the housing of the reservoir is wound round with a "Thermocoax"-type heating wire 6 capable of supplying the thermal energy necessary for the evaporation of the Cs. The temperature of the reservoir is measured by means of a chromel-alumel thermocouple 7 screwed to the end of the reservoir.

[0071] At the evaporation block exit, the Cs vapour escapes through an 8 mm hole in a stainless steel tube which also has a diameter of 8 mm and a length of 180 mm, which guides the gas towards the entry of the internal part of the evaporator. To avoid condensation of the Cs on the walls of this guide tube, the tube is wound round with a heating wire 8 lodged in grooves.

[0072] The external and internal parts are separated by a gate valve 4 enabling the evaporation block to be isolated from the main chamber 3 when the evaporator 5 is not in operation. When the evaporator is in operation, the two parts are brought back into contact with each other by moving the external part by means of a bellows-operated translator 9.

1.2.2. Internal part

[0073] The internal part of the evaporator serves to deliver the stream of neutral Cs onto the zone to be analysed in the form of a jet of sufficiently reduced diameter to avoid any contamination of the analysis chamber 3. The whole of the internal part is mounted on the main chamber of the CMS machine by means of a union 10 adjustable in distance and inclination to allow optimum positioning of the spot of Cs^0 on the useful zone. The axis of the evaporator forms an angle of 45° with respect to the normal to the sample.

[0074] When the end piece of the external part guide tube is brought into contact with the entry plate of the internal part by means of the translator 9, the Cs vapour can propagate itself in a second stainless steel tube 11 which has an internal diameter of 8 mm and is 177 mm long. At the end of this tube 11 is a metal support plate on which is mounted a motorised obturation system 12 which allows the stream of Cs^0 to be adjusted continuously between 0 and 100%, using a disc with slit of continuously variable width 16 driven by a stepper motor 17 (see figure 6).

[0075] At the exit from the obturation system 12 is located the end piece 13 of the gun which serves to further reduce the diameter of the jet of Cs^0 . This end piece is formed by stainless steel cylinder 45 mm long with an internal diameter of 5 mm which ends in a cone with an escape hole 2 mm in diameter.

[0076] All the pipes in the internal part can be heated by means of a second heating wire 14. The temperature is monitored on the end piece of the gun by means of another chromel-alumel thermocouple 15.

1.3. Characterisation

1.3.1. Thermal behaviour

[0077] Because of their different weights and environments, i.e. vacuum for the internal part, atmosphere
5 for the external part, the external and internal parts present fairly different thermal behaviours. It is thus necessary to apply a much greater power to the heating element of the external part than to that of the internal part when one wishes to raise the two tubes to the same
10 temperature. On the other hand, the fact that the external part loses a considerable proportion of the heat received to the external environment via the evaporation block and via the bellows of the translation system, the surface of which is comparable to that of a radiator, allows the
15 temperature of the reservoir to be lowered quickly with a view to stopping the evaporator.

[0078] While the internal part must be raised rapidly to a temperature of 110°C to avoid any risk of condensation and obturation in the various tubes, the
20 heating power brought to the external part should be increased in successive steps to guarantee progressive heating of the Cs reservoir.

1.3.2. Cs⁰ evaporation rates: calibration of deposition rates

25 [0079] In order to be able to measure the stream of neutral Cs delivered by the evaporator, a quartz microbalance system was installed on the CMS machine. The measuring device consists of a Leybold Inficon sensor equipped with a quartz crystal covered with a layer of gold
30 and with a working frequency of 6 MHz. Using a Leybold Inficon XTM/2 deposition monitor and after a careful calibration taking into account the adhesion of the Cs film

deposited on the quartz, we thus manage to determine the stream of Cs^0 with an accuracy of 0.01 \AA/s , which is equivalent to a deposition rate of approximately $4 \cdot 10^{-3}$ monolayers per second.

5 **[0080]** The sensor is installed by means of two tubes on a translation system occupying a flange of the main chamber on the side diagonally opposite the evaporator (not shown). This assembly enables the sensor to be moved on a horizontal axis located at the same distance from the
10 extraction optics as the sample during the analyses. Thus the sensor can be brought in front of the stream of Cs^0 at the point where the sample is normally positioned and can be removed to be replaced by the sample-holder for the analyses. In addition, the system set up enables a profile
15 to be produced through the jet of Cs^0 by sweeping the diagonal of the beam with the sensor.

[0081] Figures 7 and 8 represent the calibration curves enabling the stream of Cs^0 to be adjusted by adapting the heating power of the reservoir. Independently
20 from the power P_{ext} applied, the internal part of the evaporator is raised during all the analyses to 110°C . From these calibration curves it can be concluded that Cs^0 deposition rates on the sample of the desired order of 1 \AA/s can be reached with reasonable heating powers and
25 temperatures.

[0082] As curves 7 and 8 exhibit an exponential change in the deposition rate as a function of the heating power P_{ext} applied to the reservoir and of the temperature of the reservoir, even greater flow rates appear possible
30 by increasing the temperature by only a few degrees.

[0083] Finally, we should note that the heating and evaporator flow rate stabilisation phases result in a time of approximately 90 min. to reach a deposition rate of 1 \AA/s after start-up of the evaporator.

1.3.3. Pressure conditions

[0084] The reservoir temperature range (70 °C to 90 °C) required for the evaporator to output the necessary flow corresponds according to the Cs saturating pressure curve to a pressure range in the source of between $1 \cdot 10^{-4}$ mbar and $4 \cdot 10^{-4}$ mbar. This value appears to be realistic in view of the length (approximately 40 cm) and the small diameter (between 2 mm and 8 mm) of the pipe connecting the reservoir to the main chamber through which the pumping is carried out.

[0085] In addition, we observe that the pressure in the analysis chamber remains at a quite acceptable level during the operation of the evaporator ($4 \cdot 10^{-8}$ mbar to $1 \cdot 10^{-7}$ mbar for deposition rates between 0.3 Å/s and 3.5 Å/s).

1.3.4. Stability of deposition rates

[0086] By recording the deposition rates indicated by the microbalance controller for various heating powers and therefore for different values of the evaporator flow rate (see example in figure 9 for $P_{\text{ex}} = 85$ W), we determined a deposition rate stability $\Delta v_D / v_D = 2\%$ over 60 min.

1.3.5. Dimensions of Cs^0 beam

[0087] To evaluate the diameter of the spot of Cs^0 on the sample, we measured the deposition rate with the quartz balance for various heating powers, while moving the quartz balance on its horizontal axis using the translation system (see example in figure 10).

[0088] A first method for judging the diameter of the spot of Cs^0 produced consists in approximating the profile of the beam with a Gaussian. In this case, we obtain an average curve width of 7.5 mm. By choosing the width at mid-height as a criterion, the diameter of the

spot can be evaluated at 8.7 mm. Finally, the average width at the base of the profile ($v_D = 0$) is 18.5 mm.

[0089] Given the dimensions of the sample holder (10 cm x 7.5 cm), we can conclude that the whole stream of Cs^0 delivered by the evaporator remains confined on this plate and that there is consequently no reason to fear contamination of the analysis chamber.

[0090] In addition, the beam profiles formed made it possible to verify that the maximum Cs^0 intensity lies directly below the extraction nose of the secondary optics, which means that the spot is correctly centred on the zone to be analysed.

1.3.6. Purity of Cs^0 deposit

[0091] The cleanliness of the Cs deposit is a crucial point for the use of the Cs^0 evaporator during the analyses. A contamination of the Cs vapour with impurities would lead to an increase in the detection limits for certain elements given that the signal of the element in question would be affected by a background noise of varying degrees of intensity.

[0092] An elementary analysis of the layer of Cs deposited was carried out by two different means. First, samples of Si and AsGa exposed to the stream of Cs^0 were bombarded with Ga^+ ions and it was thus possible to record mass spectra *in situ*. Secondly, at the end of these experiments, the sample of Si used was taken out of the CMS machine to be studied on the Leica 430i Scanning Electron Microscope (LEO), given that the difference in mass between Cs (133 a.m.u.) and Si (28 a.m.u.) ought to guarantee a good contrast in electronic imaging. An EDX spectrum was notably produced in this second analysis.

[0093] The spectra obtained in SIMS analysis and in SEM analysis were compared with spectra of the same type

produced beforehand on the untouched Si and AsGa samples. This comparison shows that the mass spectra produced while the evaporator was depositing Cs on the surface are composed of the same peaks as the spectra of the untouched samples plus the typical peaks (Cs^+ , Cs_2^+ , GaCs^+ together with SiCs^+ or AsCs^+) due to the presence of Cs atoms on the samples of Si or AsGa. However, there is no explicit trace of any contaminant. We observe for example in this context that the peaks of the alkaline elements Na and K which might feature among the impurities contained in the Cs bulb do not come out at significantly higher intensities.

[0094] As regards the EDX spectra, we can note that the spectrum recorded after the deposition comprises a fairly clear peak of O. This could be explained by the fact that the Cs deposited on the sample reacted with the ambient air during the transfer of the sample between the CMS instrument and the SEM to form Cs oxides.

[0095] In the light of these results, we can conclude that the Cs deposition at typical rates around 1 Å/s does not lead to any detectable major contamination which might hinder the analyses carried out under standard Ga^+ bombardment conditions.

2. Experimental procedure

2.1. Principle

2.1.1. Characteristic parameter τ

[0096] The Cs concentration is adjusted by means of the ratio between the current delivered by the analysis beam, which was for test purposes a beam of Ga^+ ions, and the quantity of Cs deposited by the evaporator.

[0097] To characterise the analysis conditions, we define the parameter τ expressing the ratio between the

stream of Cs^0 and the Ga^+ current by means of the deposition rate v_D and the erosion rate v_{er} :

$$\tau = \frac{v_{er}}{v_D} \quad (1)$$

[0098] Qualitatively, we can therefore now assert
 5 that the Cs concentration (c_{Cs}) and the parameter τ vary in opposite directions. The greater τ becomes, the more the quantity of sputtered matter increases and the lower the proportion of Cs becomes.

2.1.2. Cs concentration produced

10 **[0099]** Let us consider a sample of density ρ_M . If we designate by Y the sputtering yield characterising the primary bombardment conditions for the type of sample considered and by ρ_{Cs} the atomic density of the layer of Cs formed, the Cs concentration can be written:

15
$$c_{Cs} = \frac{1}{1 + (\tau - 1) \cdot \frac{\rho_M}{\rho_{Cs}} + \frac{\tau}{Y}} \quad (2)$$

[0100] It is important to note that, according to the relationship above, the Cs concentration depends on the characteristics of the sample analysed -by way of its density ρ_M and its characteristic sputtering yield Y for
 20 the given bombardment conditions- together with the ratio τ between the Cs^0 erosion and deposition rates, but not the values in themselves of these two rates.

2.2. Experimental study

2.2.1. Experimental conditions

[0101] To practically test the method of analysis consisting of a Ga^+ bombardment accompanied by a deposition of Cs^0 , we used samples of aluminium, silicon and nickel, given that these materials cover a considerable range on the work function scale.

[0102] The reservoir of the Cs^0 evaporator was heated with varying powers in order to obtain different values of the deposition rate v_D .

[0103] The Ga^+ gun was operated at an energy of 28 keV and the sample polarised at + 4500 V was positioned at a distance $d = 2.5$ mm from the extraction nose. These conditions result in an angle of incidence of the primary ions of $\theta = 54^\circ$ with an impact energy of $E = 23.5$ keV.

[0104] In order to be able to vary the parameter ϕ while at the same time keeping the deposition rate constant, we changed the density of bombardment with Ga^+ ions by adapting the dimensions of the scanning surface.

[0105] A summary of the corresponding experimental conditions are given in Table 1.

| Sample holder | |
|----------------------------------|---|
| Distance | $d = 2.5 \text{ mm}$ |
| Sample voltage | $U = + 4500 \text{ V}$ |
| Ga⁺ gun | |
| Primary energy | $E' = 28 \text{ keV}$ |
| Primary current | $4.0 \text{ nA} < I_p < 4.2 \text{ nA}$ |
| Scanning surface | $38 \times 38 \text{ } \mu\text{m}^2 \text{ to } 190 \times 190 \text{ } \mu\text{m}^2$ |
| Cs⁰ evaporator | |
| Internal heating power | $P_{\text{int}} = 12 \text{ W}$ |
| Temperature of internal part | $T_{\text{int}} = 110 \text{ } ^\circ\text{C}$ |
| External heating power | $80 \text{ W} < P_{\text{ext}} < 105 \text{ W}$ |
| Temperature of external part | $75 \text{ } ^\circ\text{C} < T_{\text{int}} < 87 \text{ } ^\circ\text{C}$ |
| Deposition rate | $0.9 \text{ } \text{\AA}/\text{s} < v_D < 3,5 \text{ } \text{\AA}$ |

5

Table 1.

2.2.2. Accessible Cs concentration range

[0106] Figure 11 shows, in an example, the change in the Cs concentration determined experimentally -knowing the quantity of Cs deposited, the number of Ga⁺ ions incorporated in the volume analysed and the volume sputtered- over the given erosion rate range for four different Cs⁰ deposition rates for the aluminium sample.

[0107] To enable a comparison between these experimental values of c_{Cs} and the theoretical evolution established in the relationship, we calculated for each measurement point the ratio τ between the erosion rate and the deposition rate and plotted all the points thus obtained on the same graph.

[0108] The experimental curve of the aluminium sample resulting from this transformation operation is

20

plotted together with the respective theoretical behaviour of c_{Cs} as a function of the parameter τ in figure 12.

[0109] Several conclusions can be drawn from figure 12. First of all, the result supplied by the theoretical relationship, namely that the value of c_{Cs} depends only on the ratio between the erosion and deposition rates and not on the individual values, was corroborated experimentally. The four curves obtained for each sample when converting the erosion rate scale into a parameter τ scale are almost perfectly superimposed.

[0110] Secondly, the graphs show a very good agreement between the experimental results and the theoretical forecasts for values of τ greater than about 6. For lower values, the gap between the two curves becomes increasingly wider, while their general appearance (shape of the curve) remains generally the same. We find the same limitations concerning the area of validity of the theoretical equation (2) encountered at the time of establishment of this relationship: the theoretical forecasts are correct provided that the Cs concentration is not too great, i.e. τ does not become too small.

2.2.3. Study of useful yields attained

[0111] A systematic study clearly revealed that the useful yield -which expresses the sensitivity of the analysis- of the Cs_x^+ and MCs_x^+ clusters detected by sputtering the sample with an ion beam while simultaneously depositing neutral Cs depends solely on the ratio τ between the erosion rate and the deposition rate, but not on the values of these two rates as such (see the example in figure 13). We were therefore able to verify experimentally the following transitivity rule: given that the useful yield is a function of the Cs concentration, and as this

latter value depends on the parameter τ , the useful yield of the Cs_x^+ and MCs_x^+ clusters is a function of τ .

2.3. Comparison between the performances of the CMS instrument and those of the Cameca IMS 4f and IMS LAM

5 [0112] It is interesting to summarise in the same comparative table the maximum values of the useful yields determined above for the method of sputtering by an ion beam using a simultaneous deposit of Cs^0 and those attained for the same three samples on the Cameca IMS 4f and Cameca
10 IMS LAM instruments operated under standard conditions, namely an extraction voltage of + 4500 V and a primary energy of 10 keV (Table 2).

[0113] These three instruments use the same secondary optics and measurements have shown that the
15 transmission of these secondary optics are identical.

| <i>Sample</i> | <i>Signal</i> | <i>CMS Cs^0</i> | <i>IMS 4f/IMS LAM</i> |
|----------------------|-----------------|-------------------------------------|-----------------------|
| Al ($\Phi=4,28$ eV) | Cs^+ | $3.6 \cdot 10^{-1}$ | $3.8 \cdot 10^{-3}$ |
| | AlCs^+ | $1.3 \cdot 10^{-4}$ | $5.4 \cdot 10^{-6}$ |
| Si ($\Phi=4,85$ eV) | Cs^+ | $3.6 \cdot 10^{-1}$ | $6.5 \cdot 10^{-2}$ |
| | SiCs^+ | $1.6 \cdot 10^{-5}$ | $1.1 \cdot 10^{-5}$ |
| Ni ($\Phi=5,15$ eV) | Cs^+ | $3.6 \cdot 10^{-1}$ | $3.1 \cdot 10^{-1}$ |
| | NiCs^+ | $8.5 \cdot 10^{-5}$ | $2.0 \cdot 10^{-4}$ |

Table 2.

[0114] It can be seen that the useful yields
20 determined using a deposit of Cs^0 are higher (for materials with a low work function) and only slightly lower (for materials with a high work function) than the corresponding values obtained on conventional Cameca instruments. These differences can be explained by considering factors such as
25 the work function variations induced by the Cs deposit, the reductions resulting from the probability of ionisation of

the Cs, the cluster formation processes, the spatial and temporal correlation of the partners involved, etc.

[0115] Considering this comparison concerning the useful yields obtained together with the successful separation of the Cs sputtering and implantation stages during the analyses in MCs_x^+ mode, the potential of the Cs^0 deposit is undeniable.

2.4. Automation

[0116] Continuous recording of the secondary signals makes it possible to check at any moment that the analysis conditions are optimised, and if necessary, for example on passage from one layer to another, to adapt the stream of neutral Cs via the obturation system. The principle of this continuous and automatic optimisation is as follows.

15 [0117] By comparing the values of the various intensities at the moments t and $t+dt$, we define the value of ΔI as follows:

$$\Delta I \text{ comparator: } \Delta I = \begin{cases} 0 \\ 1 \end{cases} \text{ if } \begin{cases} I(t+dt) < I(t) \\ I(t+dt) > I(t) \end{cases}.$$

[0118] In addition, it is possible to define the opening (OPEN) of the obturator together with its variation (ΔOPEN). The value of C ("comparator") is then given by carrying out the logical operation $C = \Delta \text{OPEN} \odot \Delta I$, taking the initial condition $\Delta \text{OPEN} = 0$. Table 3 shows the corresponding logic table.

25

| $\Delta \text{ OPEN}$ | ΔI | C |
|-----------------------|------------|-----|
| 0 | 0 | 1 |
| 0 | 1 | 0 |
| 1 | 0 | 0 |
| 1 | 1 | 1 |

Table 3.

The automation programme procedure is eventually as follows:

$\Delta \text{ OPEN} = 0$

loop: calculate ΔI

$C = \Delta \text{ OPEN} \odot \Delta I$

$\Delta \text{ OPEN} = C$

[0119] The electronics of the obturator is directly coupled to the automation system and reacts to its orders:

- 5 if $\Delta \text{ OPEN} = 1$, the opening of the shutter is increased; if $\Delta \text{ OPEN} = 0$, the opening is decreased.

2.5. Conclusions

- [0120] We have shown that the analysis technique consisting of a primary bombardment with Ga^+ ions accompanied by a simultaneous deposit of Cs^0 does indeed allow the Cs concentration to be varied continuously over the whole range. The value of this range depends only on the characteristics of the material analysed and the relationship between the erosion and deposition rates, but not on the individual values of these two rates.

- [0121] Our experiments have proved that it is possible to carry out analyses in MCs_x^+ mode by sputtering the sample with a Ga^+ ion beam while simultaneously depositing neutral Cs with very promising useful yields. We have highlighted the fact that the behaviour of the Cs_x^+ and MCs_x^+ signals detected depends solely on the ratio τ between the erosion rate and the deposition rate, and not on the values in themselves of these two speeds.

- [0122] This becomes very important within the perspective of a low-energy primary bombardment with a view to an improvement of the depth resolution: in this case the sputtering yield and consequently the erosion rate take very low values; by then lowering the deposition rate to

attain optimum values of the parameter τ , we succeed in optimising the secondary signals in which we are interested.

3. EXAMPLES OF APPLICATION

5 [0123] In this section, we shall present a few examples of applications of this analysis technique. For these purposes, we shall make a distinction between the two main types of application of the SIMS technique, namely the depth profiles and ion imaging.

10 3.1. Depth profiles

3.1.1. Implant of Mg and In in Si

[0124] The sample considered consists of a silicon substrate in which magnesium and indium ions have been implanted at an energy of 300 keV and at a dose of 10^{15} atoms/cm².
15

[0125] As the elements involved come out well in the form of MCs⁺ clusters, a depth profile of this sample was made by recording the MgCs⁺, InCs⁺ and SiCs⁺ signals. In addition, the Cs⁺ and Ga⁺ secondary intensities were
20 measured in order to get an indication of the stability of the experimental conditions. Table 4 shows a summary of the corresponding experimental conditions

| <i>Ga⁺ gun</i> | |
|----------------------------------|---|
| Primary energy | $E' = 28 \text{ keV}$ |
| Primary current | $I_p = 4,2 \text{ nA}$ |
| Scanning surface | $S = 70 \times 70 \text{ } \mu\text{m}^2$ |

| <i>Cs⁰ evaporator</i> | |
|---|---|
| Internal heating power | $P_{\text{int}} = 12 \text{ W}$ |
| Temperature of internal part | $T_{\text{int}} = 110 \text{ }^\circ\text{C}$ |
| External heating power | $P_{\text{ext}} = 90 \text{ W}$ |
| Temperature of external part | $T_{\text{int}} = 80 \text{ }^\circ\text{C}$ |
| Deposition rate | $v_D = 1.5 \text{ } \text{\AA}/\text{s}$ |

| <i>Secondary optics</i> | |
|--------------------------------|----------------------------------|
| Sample-extraction distance | $d = 2,5 \text{ mm}$ |
| Sample voltage | $U = + 4500 \text{ V}$ |
| Diameter of zone analysed | $\psi = 42 \text{ } \mu\text{m}$ |
| Mass resolution | $M/\Delta M = 300$ |
| Energy bandwidth | $\Delta E = 130 \text{ eV}$ |

5

Table 4.

[0126] In accordance with the results established in the course of our study, we chose a primary bombardment density and a Cs^0 deposition rate such that the parameter τ is close to the optimum value ($\tau = 4.5$) for the formation of the MCs^+ clusters from a Si matrix. Indeed, the chosen experimental conditions lead to an erosion rate of $6.5 \text{ } \text{\AA}/\text{s}$, and we therefore arrive at a value $\tau = 4.3$. In practice, this value of τ is adjusted by varying the dimensions of the primary raster for a given primary current intensity and a given deposition rate, in order to position oneself at the critical threshold common to the Cs^+ and MCs^+ secondary intensities.

10

15

[0127] Figure 14 shows that our analysis technique makes it possible to obtain very good quality implantation profiles. Because of their lower mass at the same implantation energy, the Mg ions penetrated more deeply
 5 into the sample. It should also be noted that the matrix signals linked to the primary elements remain perfectly stable during the analysis.

3.1.2. *Implant of Ti and Cu in Al*

[0128] The second example consists of a sample of
 10 aluminium in which titanium and copper ions were implanted at an energy of 180 keV and at a dose of 10^{16} atoms/cm².

[0129] Once again, all the interesting elements can be detected in the form of MCs⁺ clusters and therefore the
 TiCs⁺, CuCs⁺ and AlCs⁺ signals were measured together with
 15 Cs⁺ and Ga⁺ as a function of time.

[0130] As a result of its low work function, the aluminium matrix reacts much more critically to the Cs deposit than is the case for Si. Consequently, and in accordance with the results established during our
 20 experimental study of the formation of the MCs_x⁺ clusters, we set the parameter τ to a higher value.

[0131] By adapting the dimensions of the primary raster to position ourselves at the critical threshold common to the Cs⁺ and MCs⁺ secondary intensities, we arrive
 25 at a value of $\tau = 5.6$, which is in full agreement with the value determined as being optimal ($\tau = 5.9$) for the analysis of the MCs⁺ clusters from an Al matrix. Table 5 shows a summary of the experimental conditions.

| <i>Ga⁺ gun</i> | |
|----------------------------------|--|
| Primary energy | $E' = 28 \text{ keV}$ |
| Primary current | $I_p = 4.2 \text{ nA}$ |
| Scanning surface | $S = 65 \times 65 \text{ }\mu\text{m}^2$ |

| <i>Cs⁰ evaporator</i> | |
|---|---|
| Internal heating power | $P_{\text{int}} = 12 \text{ W}$ |
| Temperature of internal part | $T_{\text{int}} = 110 \text{ }^\circ\text{C}$ |
| External heating power | $P_{\text{ext}} = 90 \text{ W}$ |
| Temperature of external part | $T_{\text{int}} = 80 \text{ }^\circ\text{C}$ |
| Deposition rate | $v_D = 1.5 \text{ }\text{\AA}/\text{s}$ |

| <i>Secondary optics</i> | |
|--------------------------------|---------------------------------|
| Sample-extraction distance | $d = 2.5 \text{ mm}$ |
| Sample voltage | $U = + 4500 \text{ V}$ |
| Diameter of zone analysed | $\Psi = 42 \text{ }\mu\text{m}$ |
| Mass resolution | $M/\Delta M = 300$ |
| Energy bandwidth | $\Delta E = 130 \text{ eV}$ |

5

Table 5.

3.1.3. Implant of F and Al in InP

[0132] While we exclusively measured MCs^+ type signals in the two first depth profiles, we chose for this third example a sample of InP in which we implanted both an electropositive element, in this case Al, which is analysed in the form of MCs^+ clusters and an electronegative element, namely F, which is best detected in the form of MCs_2^+ clusters. The Al implantation energy was 180 keV while that of the F was reduced to 130 keV because of its lower atomic mass. The implanted doses were set at 10^{16} atoms/cm² for the two elements.

10

15

[0133] For this depth profile, it is therefore required to record MCs^+ and MCs_2^+ type ions together with

the Cs^+ , Cs_2^+ and Ga^+ secondary signals which serve as indicators of the stability of the analysis conditions. Taking into account that the optimum values of τ depend on the particular type of secondary ion considered (Cs^+ , Cs_2^+ , MCS^+ , MCS_2^+), we cannot simultaneously optimise all the signals and we are therefore obliged to compromise concerning the setting of the parameter τ . After experimentally determining the optimum τ values for the MCS^+ ions (AlCS^+ , InCS^+ , PCs^+) and for the FCs_2^+ clusters by way of variations of the dimensions of the primary raster, we set the final value of τ for our analysis at an intermediate value ($\tau = 7.5$) leading to major secondary intensities for all the signals under interest. Table 6 shows a summary of the corresponding experimental conditions.

| <i>Ga⁺ gun</i> | |
|----------------------------------|---|
| Primary energy | $E' = 28 \text{ keV}$ |
| Primary current | $I_p = 4.2 \text{ nA}$ |
| Scanning surface | $S = 112 \times 112 \text{ } \mu\text{m}^2$ |

| <i>Cs⁰ evaporator</i> | |
|---|---|
| Internal heating power | $P_{\text{int}} = 12 \text{ W}$ |
| Temperature of internal part | $T_{\text{int}} = 110 \text{ }^\circ\text{C}$ |
| External heating power | $P_{\text{ext}} = 90 \text{ W}$ |
| Temperature of external part | $T_{\text{int}} = 80 \text{ }^\circ\text{C}$ |
| Deposition rate | $v_D = 1.5 \text{ } \text{\AA}/\text{s}$ |

| <i>Secondary optics</i> | |
|--------------------------------|-----------------------------|
| Sample-extraction distance | $d = 2.5 \text{ mm}$ |
| Sample voltage | $U = + 4500 \text{ V}$ |
| Diameter of zone analysed | $\Psi = 23 \text{ m}$ |
| Mass resolution | $M/\Delta M = 300$ |
| Energy bandwidth | $\Delta E = 130 \text{ eV}$ |

5

Table 6.

[0134] We observe in figure 16 that all the matrix signals (PCs^+ and InCs^+) together with those linked to the primary elements (Cs^+ , Cs_2^+ and Ga^+) take approximately 90 seconds to stabilise. This initial instability should

10 indicate the existence of a quite considerable transient state for this type of material, which is sputtered very easily.

[0135] Concerning the two elements implanted, we observe again that the implantation profiles recorded are

15 of very good quality.

3.2. Ion imaging

[0136] To demonstrate the possibility of producing ion images in MCS_x^+ mode by scanning the surface of the

sample with a fine Ga^+ ion beam while simultaneous depositing Cs^0 atoms on it, we recorded images of a grid by successively detecting four different elements (figure 17).

[0137] The chosen grid consists of a substrate of aluminium incorporating copper bars $5\text{ }\mu\text{m}$ wide at $20\text{ }\mu\text{m}$ intervals.

[0138] Given that the enlargement of the ion image directly depends on the dimensions of the primary sweep and that strong secondary intensities are not required, the parameter τ is not optimised in this example. Table 7 shows a summary of the corresponding experimental conditions

| <i>Ga⁺ gun</i> | |
|----------------------------------|---|
| Primary energy | $E' = 28\text{ keV}$ |
| Primary current | $I_p = 600\text{ pA}$ |
| Scanning surface | $S = 38 \times 38\text{ }\mu\text{m}^2$ |

| <i>Cs⁰ evaporator</i> | |
|---|--|
| Internal heating power | $P_{\text{int}} = 12\text{ W}$ |
| Temperature of internal part | $T_{\text{int}} = 110\text{ }^\circ\text{C}$ |
| External heating power | $P_{\text{ext}} = 75\text{ W}$ |
| Temperature of external part | $T_{\text{int}} = 75\text{ }^\circ\text{C}$ |
| Deposition rate | $v_D = 0.6\text{ }\text{\AA}/\text{s}$ |

| <i>Secondary optics</i> | |
|--------------------------------|--------------------------------|
| Sample-extraction distance | $d = 2.5\text{ mm}$ |
| Sample voltage | $U = + 4500\text{ V}$ |
| Mass resolution | $M/\Delta M = 300$ |
| Energy bandwidth | $\Delta E \approx 5\text{ eV}$ |

Table 7.

[0139] By detecting the CuCs^+ and AlCs^+ secondary ions, we manage to display only the bars forming the grid and the areas bounded by these bars. However, if we record

the Cs^+ or Cs_2^+ signals, we obtain a contrast image in which the areas between the bars appear to be raised.